*Materials Research*. 2025; 28(suppl. 1): e20250095
DOI: https://doi.org/10.1590/1980-5373-MR-2025-0095

# Technological Characterization of Clay and Chamotte Incorporated in Handmade Ceramics

**Dayana Rosy Souza dos Santos[a], Oscar Jesus Choque Fernandez[a], Diogo Monteiro Porfírio[b*], Marison Franco Rocha de Lima[b], Ramon Sousa dos Santos[b], Patrícia Magalhães Pereira Silva[c]**

[a]*Instituto Federal do Pará, Programa de Pós-Graduação em Engenharia de Materiais, Belém, PA, Brasil.*
[b]*Instituto Federal do Pará, Faculdade de Engenharia de Materiais, Belém, PA, Brasil.*
[c]*Instituto SENAI de Inovação em Tecnologias Minerais, Belém, PA, Brasil.*

Received: January 10, 2025; Revised: May 22, 2025; Accepted: June 29, 2025

The municipality of Bragança, Pará, Brazil, is renowned for its artisanal ceramic production, where chamotte is reused as a substitute for clay materials. In this study, test specimens were formulated and produced with clay partially replaced by chamotte in proportions ranging from 0% to 25%, and sintered between 600°C to 1000°C. Both the clay and chamotte underwent technological characterization. The specimens were subjected to physical and mechanical analyses. The raw materials consist of quartz, illite, kaolinite, and K-feldspar, with $SiO_2$ and $Al_2O_3$ as the predominant chemical components. The clay is clayed silt, exhibits an appropriate plasticity index, and undergoes structural transformations as the temperature increases, confirming its suitability for ceramic applications. The best results were obtained with 5% to 15% chamotte in ceramics sintered at 900°C, reaching a mechanical strength of 7 MPa. The data on various technological properties indicate the feasibility of producing artisanal ceramics incorporating chamotte.

**Keywords:** *Handmade ceramics, Waste, Recycling.*

## 1. Introduction

Clays and clay-based materials are naturally abundant, readily available, and inherently non-polluting[1]. These materials have been employed by humans since the earliest stages of technological advancement, primarily due to their favorable thermal stability and mechanical resistance[2]. The manufacture of artisanal ceramics from natural clays deeply rooted in human history and closely associated with the evolution of the ceramic craftsman[3]. The Brazilian ceramic industry is composed of approximately 13.084 enterprises, underscoring its strategic relevance within the national economy[4]. Annual production statistics attest to the sector's magnitude: 2.35 billion ceramic tiles, 5.76 billion ceramic blocks, and 236.844 tons of ceramic accessories are produced each year. The combined output of blocks and tiles thus surpasses 8.35 billion units annually, evidencing the sector's critical role in supplying construction materials[5]. Despite such scale, the practice of ceramics, particularly in Brazil's interior regions, often remains grounded in intuitive knowledge of clay behavior, owing to limited access to advanced infrastructure and technological resources. Nonetheless, the judicious selection and combination of raw materials enable the development of ceramic products with improved quality, reliability, and performance. Brazil ranks as the third largest global producer and consumer of red ceramics, which has resulted in a substantial body of scientific literature dedicated to clay materials and their applications[6]. However, the characteristics of clays are highly dependent on their geological origin, leading to considerable variability in their physical, chemical, and mineralogical properties. In this context, systematic characterization studies are essential to elucidate the industrial potential of specific clay deposits. Such studies contribute not only to the optimization of extraction and processing routes but also to the identification of novel, high-value applications in advanced ceramics and related fields[7].

The clays originating from the municipality of Bragança in the state of Pará, Brazil, are traditionally recognized for their use in the artisanal production of refractory materials, utilizing extracted clay from local clay deposits[8,9]. Despite this longstanding tradition of handcrafted ceramic manufacturing, it remains largely underexplored in terms of systematic scientific research aimed at characterizing the raw materials employed in these processes. Additionally, due to the high volume of ceramics production in the region a substantial amount of sintered ceramic waste, primarily in the form of fractured or defective pieces, is continuously generated and subsequently discarded. Once this waste is ground into a fine particulate, it is commonly referred to as chamotte.

Chamotte is a refractory ceramic material produced by firing selected fire clays at elevated temperatures[8], often found in production of ceramic refractory pieces as broken pieces that are grinded to a powder. It typically contains a high proportion of alumina ($Al_2O_3$) and silica ($SiO_2$)[9]. Industrially, chamotte is produced by firing fire clays in a

*e-mail: mdiogo610@gmail.com
**Associate Editor**: Eliana Muccillo.
**Editor-in-Chief**: Luiz Antonio Pessan.

rotary kiln, then grinding and screening the resulting material to specific particle sizes[10,11]. Chamotte has properties of high refractoriness due to its high $Al_2O_3$, low porosity achieved through quality firing, angular particles that fill space effectively in shaping operations[12,13]. Used in various ceramic products such as refractory bricks, blocks, tiles, castables, foundry molds, sanitary ceramics, and ceramic mixtures. Often used as a filler in tile manufacture and even slipcast products, chamotte is also called grog or firesand[12,14].

Generally, technological studies on handmade ceramics incorporating chamotte are scarce and lack standardizations, unlike those conducted on industrial ceramics, which typically follow well-established methodologies and quality protocols. This gap underscores the need for systematic investigation in the context of artisanal ceramic production. Therefore, the present study aims to conduct a comprehensive technological characterization of raw materials, with a particular focus on determining optimal formulations for production of handcrafted refractory cookware incorporating chamotte. The objective is twofold: first, to provide scientific and technical support to the artisanal ceramics community, enhancing the quality and consistency of their products; and second, to demonstrate the potential for chamotte reuse as a valuable recycled material, aligning with sustainable practices in ceramic processing.

## 2. Experimental

### *2.1. Raw material*

The material samples were obtained from the São Mateus community in the municipality of Bragança, located in the state of Pará, Brazil. This region has clay resources that are extracted for use in local brick, tile, and ceramic handicraft sectors. Clay blocks measuring 14.5 x 14.5 x 22.5 cm in dimension (Figure 1a) and 15 kg of chamotte (Figure 1b) were collected from the *Artesanato Panela de Barro*, handmade ceramics shop in Bragança. The clay is processed and cleaned to remove organic residues and possible coarse particles. The artisans mix and homogenize it manually to remove air bubbles from inside the block; this activity may cause future problems related to the firing of the pieces. The clay samples were disaggregated in a knife mill and sieved through a 100-mesh sieve to obtain a homogeneous fine fraction smaller than 150 microns in size. The chamotte sample is a product of discarded ceramic pots fired at approximately 1000°C. It is left exposed at the pottery workshop and is subject to contamination by material from the work environment. The material, which is reused by the artisans, is crushed with a hammer and then pounded in a mortar until it becomes very fine powder. The fragmented chamotte was sieved through 80# mesh (0.177 mm) to obtain a uniform particle size distribution for the preparation of the test specimens. The clay and chamotte samples were subjected to granulometric studies to determine the respective dosages for the test specimens.

### *2.2. Methods*

#### *2.2.1. Mineralogical analysis*

The mineralogical composition of the raw material phases was determined by X-ray diffraction (XRD), using an Empyrean/PANalytical diffractometer equipped with a Co radiation source ($K_{\alpha 1}$ = 1.78901 Å, converted to Cu $K_{\alpha 1}$), operating at 1.8 kW. The analysis conditions were as follows: 40 kV and 40 mA; θ–θ goniometer; scanning range from 5° to 70° (2θ); line focus; $Fe_{K\beta}$ filter; 0.04 rad Soller slits; 1/4° divergence slit and 1/2° anti-scatter slit; 10 mm mask; step size of 0.026° (2θ); 1 revolution per scan; and a PIXcel3D 1x1 detector. The HighScore Plus software was used to identify samples in the XRD by comparison with files of the standard Powder Diffraction File (PDF). The samples were prepared using the backloading method.

#### *2.2.2. Chemical analysis*

The chemical composition of the raw material was carried out on a Bruker S2 Ranger X-ray fluorescence (XRF) spectrometer with a Pd tube operated at 60 kV. The analyses were carried out on pressed pellets prepared with 1:3 binder-to-sample ratio using WAX. Loss on Ignition (LOI) tests were also performed.

#### *2.2.3. Thermal analysis*

To study the thermal variations of clay and chamotte when subjected to high temperatures, thermogravimetric analysis (TG) was performed to determine mass loss, and differential scanning calorimetry (DSC) to determine thermal behavior.

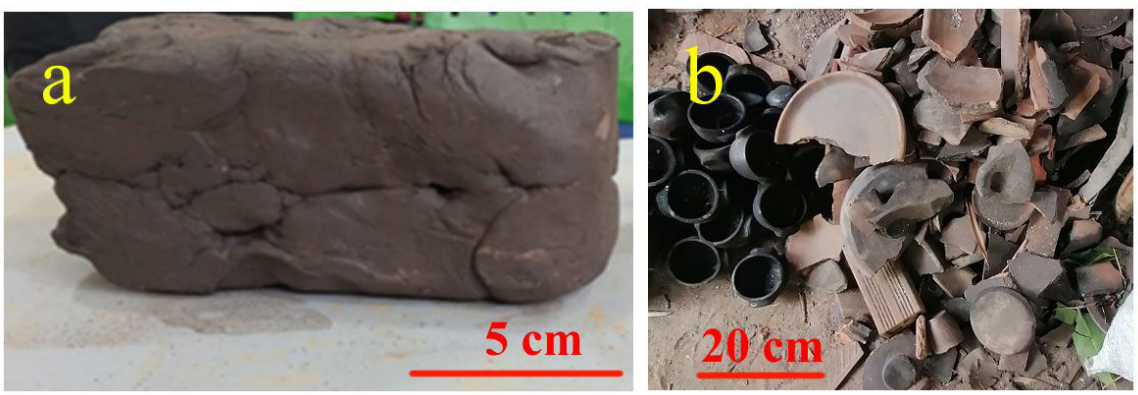


**Figure 1.** a) Clay block and b) chamotte.

A simultaneous thermal analyzer (TG/DSC), model STA 449 F3 Jupiter from Netzsch, was used. Approximately 30 mg of the powdered sample was subjected to a temperature ramp from 25 to 1000 °C at a heating rate of 10 °C/min, under a nitrogen ($N_2$ 5.0) flow of 70 mL/min, using a Pt/Rh crucible in a vertical cylindrical SiC furnace.

### *2.2.4. Physical tests*

Granulometric analysis was carried out via laser diffraction granulometry, from the Malvern, model Mastersizer 3000. Analysis variables: Agitation = 2500 rpm; without Ultrasound; Density = 1.56 g/cm$^3$; RB Refractive Index = 2.25; Absorption Index = 0.1; Dispersant = distilled water and Refractive Index of the Dispersant = 1.39. The determination of the density of the clay and chamotte samples was performed using pycnometry, for this the samples were dried in an oven at 100°C, and subsequently disaggregated in an agate mortar to obtain fractions smaller than 2 mm. The Atterberg Limits were determined according to the procedure specified in NBR 6459[15] for the Liquid Limit and NBR 7180[16] for the Plastic Limit, or alternatively, in accordance with ASTM D4318-17[17].

### *2.2.5. Production and ceramic properties of prismatic samples*

For characterization of ceramic production and the incorporation of chamotte into the clay material matrix, five test specimens measuring 100 x 50 x 10 mm were produced for statistical variance, with varying mass proportions of chamotte incorporation (0%, 5%, 10%, 15%, 20%, and 25%) (Table 1). These incorporations levels were selected based on the traditional practice of potters and artisans from São Mateus, who typically use 10% chamotte in a 90% clay mixture.

After 14 days of drying, a thermal cycle was applied to the prismatic samples using a muffle furnace. A thermal program consisted of three stages: heating at 100˚C for 2 hours, followed by 1 hour of heating at an intermediary temperature of 400°C then heating to the target sintering temperature (ranging from 600°C - 1000°C). Finally, the prismatic samples were allowed to cool naturally inside the muffle furnace. Various physical properties of the prepared samples were evaluated, including water absorption (WA), apparent porosity (AP), and bulk density (BD), with the results interpreted according to Brazilian standards NBR (ISO) 10545-3[18]. The Linear Firing Shrinkage (LFS) was determined in accordance with ASTM C326-09[19] and the literature[20,21].

### *2.2.6. Mechanical tests*

Flexural Strength tests were conducted to evaluate the strength of the test specimens with different material concentrations. Three specimens were tested for each mixture at temperatures of 600°C, 700°C, 800°C, 900°C, and 1000°C, with chamotte incorporation levels of 0%, 5%, 10%, 15%, 20%, and 25%, totaling 90 test specimens. A universal testing machine was used in three-point bending mode, with a speed of 1 mm/min and a support span of 70 mm. Each specimen was subjected to an increasing load at the midpoint until failure. The test was performed utilizing the INTEMERTRIC electromechanical universal testing machine iM-50. During the test, the machine automatically recorded force and displacement values, enabling the generation of stress-strain curves for each concentration. The test was performed according to the ASTM C674-88[22] standard, and the collected data were processed to calculate the rupture stress and modulus of elasticity. Statistical analyses, including mean, standard deviation, and confidence intervals, were performed to provide a detailed overview of the results.

**Table 1.** Clay:chamotte proportion in the production of test specimens.

| Clay:chamotte (%) | Ceramic firing temperatures (˚C) |
|---|---|
| 100:0 | 600, 700, 800, 900, 1000 |
| 95:05 | 600, 700, 800, 900, 1000 |
| 90:10 (Reference) | 600, 700, 800, 900, 1000 |
| 85:15 | 600, 700, 800, 900, 1000 |
| 80:20 | 600, 700, 800, 900, 1000 |
| 75:25 | 600, 700, 800, 900, 1000 |

### *2.2.7. Morphological test*

Morphological analyses of the clay and chamotte materials, as well as on the fracture surfaces of the test specimens, were performed using Scanning Electron Microscopy (SEM) coupled with Energy Dispersive System (EDS), VEGA 3 LMU model from TESCAN. For sample preparation, the test specimens, previously dried and fractured during mechanical testing, were placed in a desiccator. Millimetric fragments were collected from the fractured surface and mounted on a stub. The fragments were then gold coated.

## 3. Results and Discussion

### *3.1. Mineralogical, chemical and thermal characterization*

The clay material is composed of quartz ($SiO_2$), kaolinite $Al_2Si_2O_5(OH)_4$, and illite $KAl_2Si_3AlO_{10}(OH)_2$ (Figure 2a). The presence of the latter phase was confirmed by the diffraction peaks at (002) (8.87°), (110) (19.84°), (006) (26.83°), and (131) (35.02°).This mineralogical proportion is inferred from the peaks of high crystallinity of quartz compared to kaolinite and illite. Similar results for quartz, kaolinite and illite are reported in other studies, classifying it as a kaolinitic clay[13,23-26]. The chamotte sample shows high-crystallinity quartz ($SiO_2$), along with illite and microcline ($KAlSi_3O_8$). The absence of kaolinite is attributed to the fact that the chamotte has already undergone firing at elevated temperatures, resulting in the loss of kaolinite's crystallinity above 600 °C. In contrast, the presence of illite and feldspar is characteristic of the working environment of the pottery workshop. Similar mineralogical profiles, particularly the presence of quartz and illite, have also been reported in other chamotte samples[12,27].

The SEM micrographs of the raw materials are shown in Figure 3. The clay sample (Figure 3a) exhibits a texture with an irregular surface and micrometric aggregates, and it is morphologically homogeneous. The EDS spectrum of the mapped area (not shown) indicates the presence of silicon and aluminum in high concentrations, as well as potassium, iron, and oxygen. These elements are consistent with the typical composition of clay minerals such as kaolinite, illite, and quartz, confirming the predominantly aluminosilicate nature of the clay, characteristic of the quartz and silicates previously identified by XRD in Figure 2a.

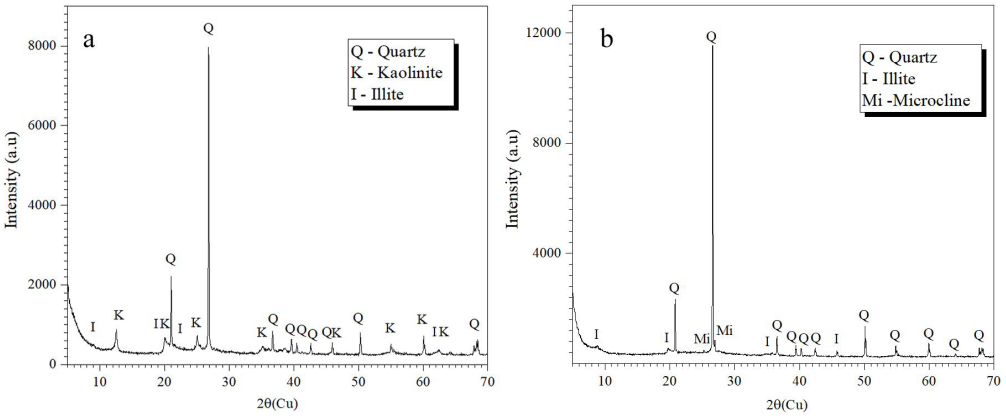


**Figure 2.** X-ray diffraction pattern: a) clay material, b) chamotte. Quartz: PDF: 01-087-2096; Kaolinite: PDF: 00-029-1488, Illite: PDF: 00-002-0056, Microcline: PDF: 01-0710955.

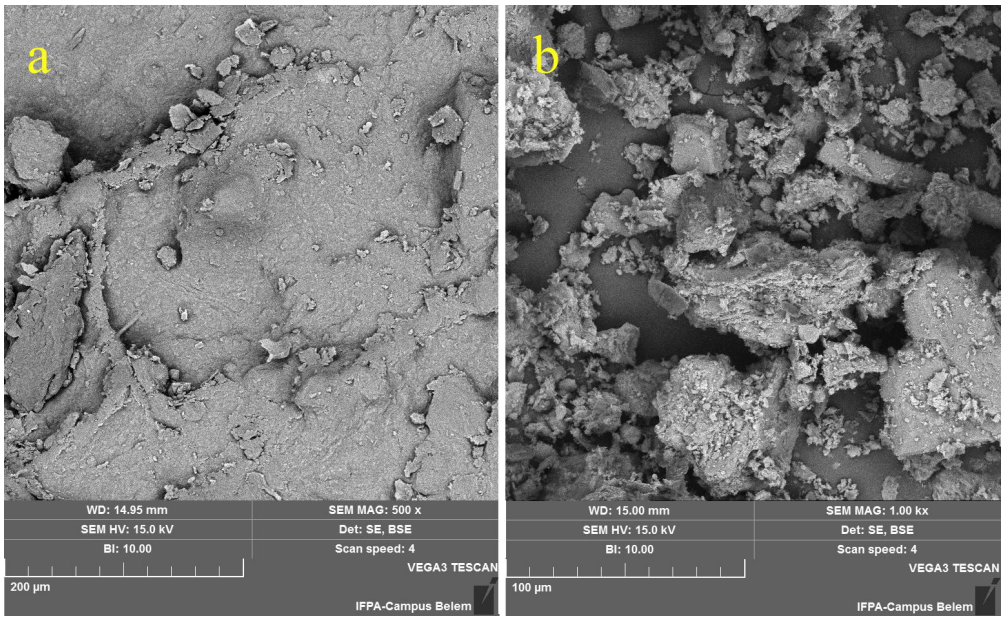


**Figure 3.** SEM micrographs of the raw materials: a) clay; b) chamotte.

For the chamotte sample (Figure 3b), grains with irregular contours and varying sizes can be observed. On the surface of these grains, fine aggregates of clay material or even fine chamotte are present. The grain size, reduced by the pottery workshop process, differs substantially from that of the clay, suggesting the need for particle size control when used in mixtures. The EDS spectrum of the mapped area is similar to that of the clay sample, though with differing concentrations of silicon and aluminum, as well as potassium, iron, and oxygen, confirming the results obtained by XRD (Figure 2b).

Chemically the clay material presents major concentrations of silicon oxide (58.19%), aluminum oxide (21.28%), and iron oxide (4.99%) (Table 2). Titanium, magnesium, and potassium oxides are present in lower concentrations. These oxides are typically associated with aluminosilicates, such as kaolinite and illite[24,27], identified by XRD. The latter mineral occurs at approximately 7% in the clay material, estimated from the $K_2O$ content and assuming that all the potassium is present in this phase. The titanium oxide corresponds to anatase, although in quantities too low to be detected by XRD. In the chamotte sample, the oxides with the highest concentrations are silicon oxide (63.16%), aluminum oxide (21.32%), and iron oxide (7.02%), along with titanium, magnesium, and potassium oxides. The titanium oxide corresponds to rutile, as result of the transformation from anatase; however, it is present in quantities below the detection limit of XRD. When comparing the oxides compositions of both materials, no significant differences are observed, which corroborates the inference that the chamotte is produced from the same raw materials as the clay[23,27].

Thermal analysis carried out on the raw material shows that clay sample (Figure 4a) exhibits an initial mass loss of approximately 3% between 60°C-100°C, corresponding to the evaporation of physically adsorbed moisture. A second loss of 8.0% occurs in the range of 400°C – 600°C, which is typical for materials

**Table 2.** Chemical composition of clay and chamote compared with other materials reported in the literature.

| | MgO % | $Al_2O_3$% | $SiO_2$% | $SO_3$% | $K_2O$ % | CaO % | $TiO_2$% | $Fe_2O_3$% | LOI % | Total % |
|---|---|---|---|---|---|---|---|---|---|---|
| Clay Bragança | 1.82 | 21.28 | 58.19 | 0.33 | 1.19 | - | 1.19 | 4.99 | 11.0 | 100.00 |
| Chamotte Bragança | 1.62 | 21.32 | 63.16 | 0.27 | 1.38 | 0.11 | 1.52 | 7.02 | 3.50 | 100.00 |
| Red clay[27] | 0.32 | 21.38 | 63.25 | 0.12 | 1.82 | 2.15 | 1.12 | 6.18 | 6.12 | 100.00 |
| Clay[24] | 0.13 | 25.89 | 62.19 | - | 0.78 | 0.13 | 1.01 | 0.67 | 9.10 | 100.00 |
| Tile[23] | 0.80 | 20.80 | 65.70 | - | 3.63 | 0.35 | 1.04 | 6.28 | 2.05 | 100.00 |
| Chamotte[28] | 0.97 | 25.36 | 55.98 | - | 2.24 | 0.37 | 1.32 | 9.57 | 3.30 | 100.00 |

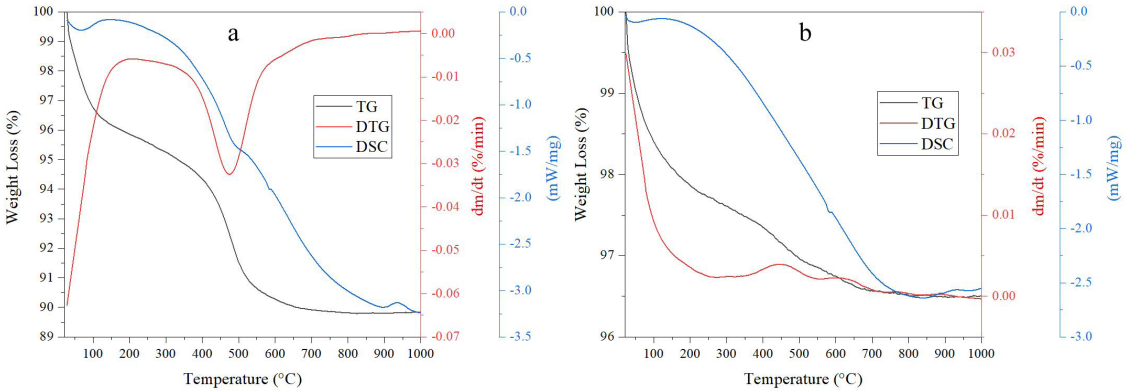


**Figure 4.** TG, DTG and DSC curves: a) clay, b) chamotte.

containing clay minerals such as kaolinite[23,26,29] and illite, due to the loss of structural OH groups and consequent release of water molecules. The total mass loss observed was 11%, which is also corroborated by the LOI data in table 2. The DTG curve shows the thermal decomposition range of kaolinite and illite, with mass loss occurring between 400°C - 700 °C[30,31]. Three endothermic peaks and one exothermic peak, although not clearly defined in the DSC curve were identified. The endothermic peaks are associated with moisture loss and the dehydroxylation of kaolinite and illite structures. Kaolinite transforms into a metastable and disordered metakaolin phase ($Al_2Si_2O_7$)[24,27]. Illite shows an endothermic peak at approximately 575°C, corresponding to the dehydroxylation of its crystalline lattice[32,33], which may also be attributed to the α–β quartz phase transition (~573°C)[34]. The exothermic peak at approximately 920°C, suggests recrystallization or the formation of new phases. At around 975°C, mullite nucleation begins through spinel formation. The quartz phase remains stable at these temperatures[14,23,27].

The thermal behavior of the chamotte indicates a gradual mass loss[14] (Figure 4b). Moisture loss is not very pronounced, with a decrease of approximately 1.5% occurring between 60°C- 120°C. Above this temperature range, the total mass loss reaches about 3.5%, likely due to the presence of residual clays within the chamotte. One endothermic peak and one exothermic peak, though not clearly defined in the DSC curve, were observed. The endothermic peak is associated with moisture loss. No endothermic peaks related to kaolinite are distinguishable, as corroborated by the XRD results (Figure 2). The exothermic peak, located at approximately 920°C, suggests recrystallization or the formation of new phases, including mullite[24,26,27].

## *3.2. Physical characterization*

The particle size distribution of the raw materials, clay and chamotte is presented in Figure 5 and were interpreted according NBR 7181[35] and ASTM D6913 standards[36]. Results indicate that the clay sample presents three defined granulometric fractions, classified as sand, silt, and clay (Table 3). The sample exhibited grain sizes in the sand fraction (28%), in the silt fraction (67%) and the clay (5%). Therefore, 72% of the sample consists of silt and clay. For the chamotte sample, the granulometric curve displays two granulometric fractions: sand fraction (63%), silt (35%), and clay (2%). Thus, 98% of the sample consists of sand and silt. It can be observed that the clay material is silty loam soil, while the chamotte is sandy-silty[36]. This indicates that the fragmentation of the chamotte for use in ceramics is still coarse, and it's similar to other research[12,26,28].

The density of the clay material is 2.47 g/cm$^3$, while the density of the chamotte material is 2.25 g/cm$^3$.The Atterberg tests results (Table 4) for the clay material showed that the Plastic Limit (PL) was 28%, Liquid Limit (LL) 54%, and Plasticity Index (PI) 26%. The results indicate that the material is classified as highly plastic, meaning it can be easily conformed without volume variation and worked within a broad moisture range[14,26,27,37,38].

## *3.3. Ceramic properties of prismatic samples*

The water absorption (WA) results for the sintered test specimens are shown in Figure 6a. It can be observed that

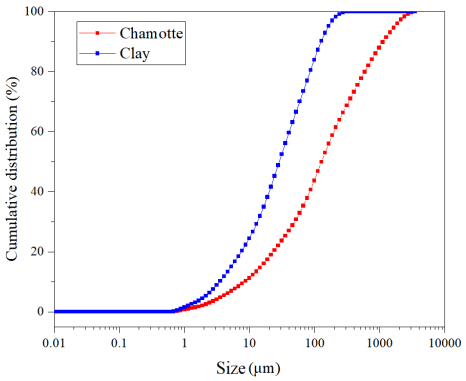


**Figure 5.** Cumulative particle size distribution curves of clay and chamotte.

**Table 3.** Granulometric proportion of the materials.

| Clay Material | (%) | Chamotte | (%) |
|---|---|---|---|
| Clay | 5 | Clay | 2 |
| Silt | 67 | Silt | 35 |
| Sand | 28 | Sand | 63 |
| Total | 100 | Total | 100 |

**Table 4.** Atterberg limits of the clay material.

| Atterberg limits | % |
|---|---|
| Plastic limit | 28 |
| Liquid limit | 54 |
| Plasticity Index | 26 |

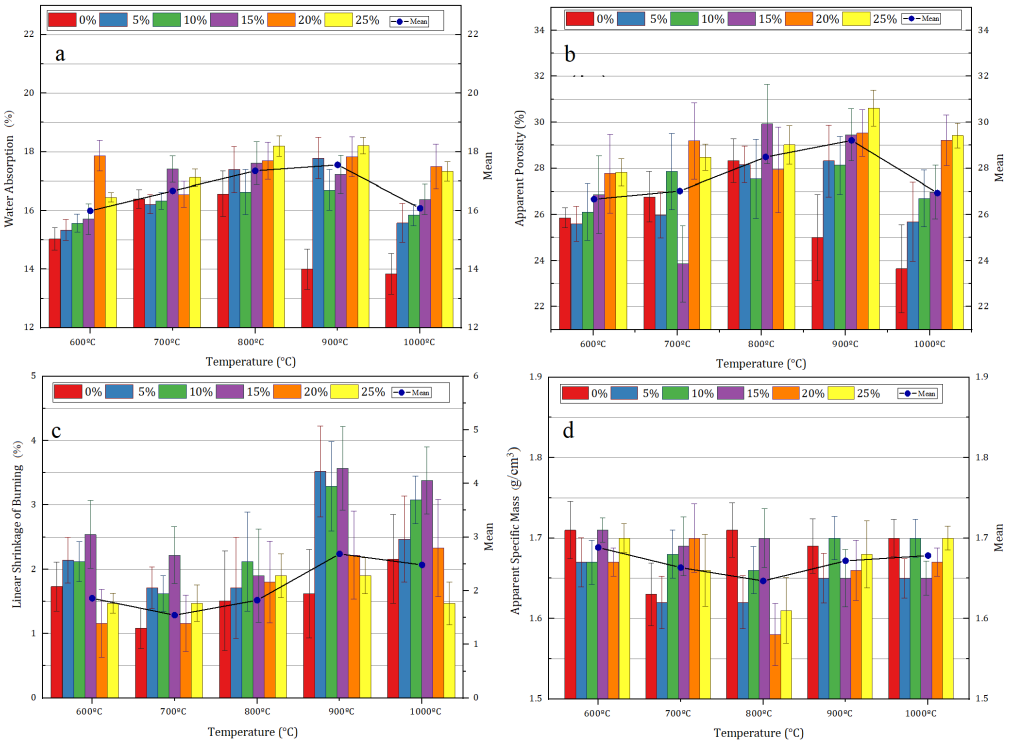


**Figure 6.** Ceramic properties of prismatic specimens as a function of sintering temperatures and chamotte content: a) water absorption, b) apparent porosity, c) linear firing shrinkage, and d) bulk density.

for each sintering temperature, there is a gradual increase in water absorption (WA), with higher WA values occurring at higher chamotte incorporations. There is also a tendency for WA to increase between 600°C -900°C, with a slight decrease at 1000°C. All results show WA values ranging from 14% to 20%, which are in accordance with the NBR-ISO 10545-3[18] standard. Is established a maximum permissible water absorption limit of 20% after firing ceramic tiles[18-21,38,39].

The apparent porosity (AP) results as a function of sintering temperature are presented in Figure 6b. A progressive increase in AP is observed from 600°C to 900°C, followed by a reduction at 1000°C. Additionally, a consistent rise in porosity is noted with increasing chamotte content, apart from the sample containing 15% chamotte sintered at 700°C. Despite this general trend, the standard deviations indicate minor but distinct variations across the dataset. The porosity increase observed between 600°C - 900°C is primarily attributed to thermal events such as dehydration and dehydroxylation of the clay matrix, affecting both the pure clay and chamotte-containing compositions[18-21,38,39]. During extrusion, residual air is trapped within the body, forming pores that persist through sintering. According to the thermal analysis shown in Figure 3a, the clay-based systems tend to stabilize around 800 °C. In this range, sintering does not significantly reduce porosity; instead, consolidation occurs predominantly through the coalescence of pores

rather than their elimination, as reported by Ducman et al.[40]. Effective densification and substantial reduction in porosity become evident only at temperatures above 900°C. Several studies report that the onset of densification and porosity closure typically begins around 850°C and progresses up to 1000°C[2,41,42]. All ceramic bodies sintered between 900°C and 1000°C exhibited porosity values below 30%, confirming a significant decrease in open porosity at elevated temperatures.

The results of Linear Firing Shrinkage (LFS) (Figure 6c) reveal a gradual increase in LFS between 600°C to 900°C, followed by stabilization up to 1000°C. This behavior indicates that 900°C corresponds to the temperature at which the maximum LFS occurs in the tested specimens. Accordingly, LFS is relatively low at lower temperatures and increases progressively with the sintering temperature until 900 °C. In relation to the chamotte content, LFS increases steadily from 0% to 15%, reaching a peak at 15% addition. Beyond this point, a gradual decrease in LFS is observed from 15% to 25% chamotte content across all temperatures. These findings suggest that 15% chamotte represents the optimal content for achieving maximum linear firing shrinkage in the studied compositions[18-21,38,39].

The linear firing shrinkage (LFS) observed in the test specimens is closely related to the packing density of the chamotte within the clay matrix. Lower LFS values are indicative of reduced packing efficiency, whereas higher values suggest increased compaction. From 900°C onwards, a notable increase in LFS is observed, which may be attributed to enhanced liquid phase formation due to the interaction between fluxing oxides and the clay components. This process promotes densification and reduces the porosity of the sintered bodies. As shown in Figure 6c, shrinkage remains relatively stable and within acceptable limits up to approximately 800°C. However, above 900°C, the sharp increase in linear shrinkage may pose a risk of thermal cracking during cooling. Despite this, the overall LFS values remain within the range of 1% to 3%, aligning with the recommended limits for ceramic bricks and tiles[18-21,38,39].

The bulk density results (Figure 6d), show a progressive reduction until 800°C followed by a slight further increase beyond this temperature. These results highlight the influence of thermal treatment on the densification and structural stability of the test specimens[18-21,38,39]. The increase in apparent density above 800°C is primarily attributed to a significant reduction in open porosity, as reported by Jordan et al.[41], and to thermal contraction mechanisms, as described by Hulan et al.[30]. These phenomena contribute to the compaction and consolidation of the ceramic matrix during the sintering process.

## 3.4. Flexural strength

The flexural strength results are shown in Figure 7. For samples without chamotte (0% addition), the highest strength is observed at 1000°C. As chamotte content increases, a general pattern of decreasing flexural strength is evident across all sintering temperatures. Notably, the values at 1000°C remain consistently the highest, exceeding 7.5 MPa, regardless of chamotte content. Between 600 °C and 800 °C, strength values show only slight variations with changes in temperature and chamotte concentration. In contrast, sintering at 900°C and 1000°C yields significantly improved mechanical performance, indicating that higher temperatures favor the development of stronger ceramic bodies. Although the optimal chamotte content for clay replacement is not definitively established, it can be suggested that additions between 5% and 15% sintered at 900°C represent a viable balance between mechanical strength and practical processing conditions. While the best performance is achieved at 1000°C, this temperature is generally less accessible for traditional or artisanal ceramic production. Flexural strength is closely related to the formation of crystalline phases within the ceramic matrix, which become prominent between 900°C and 1000°C. These phases, particularly silico-aluminates, contribute to improved fired strength by enhancing the rigidity and cohesion of the microstructure.

## 3.5. Micromorphology of specimens fragmented

The SEM images reveal distinct microstructural changes in the ceramic samples containing 0% chamotte over the sintering temperature range of 600°C to 1000°C. At 600°C (Figure 8), the microstructure is characterized by a relatively porous network, with loosely packed particles and minimal evidence of bonding. As the temperature increases to 700°C, a gradual densification is observed, with particles appearing more compact and exhibiting early signs of particle rearrangement. At 800°C, further densification occurs, accompanied by the initial formation of necks between adjacent particles, indicative of the onset of sintering. At 900°C, the sintering process becomes more pronounced, leading to a notable reduction in porosity and the development of a more continuous and interconnected grain structure. By 1000°C, the microstructure displays a highly densified matrix with extensive neck formation and minimal visible porosity, suggesting near-complete sintering. These microstructural changes align with the expected behavior of clay-based ceramics during thermal treatment, where progressive particle bonding and pore elimination contribute to the mechanical and physical consolidation of the material.

The SEM micrographs (Figure 9) illustrate the morphological evolution of a clay matrix with chamotte as a function of increasing chamotte content. At 0% addition, the microstructure appears relatively homogenous and compact, characteristic of a pure clay body with minimal heterogeneity. As the chamotte content increases, the surface texture becomes progressively coarser, exhibiting well-defined agglomerates and angular chamotte particles

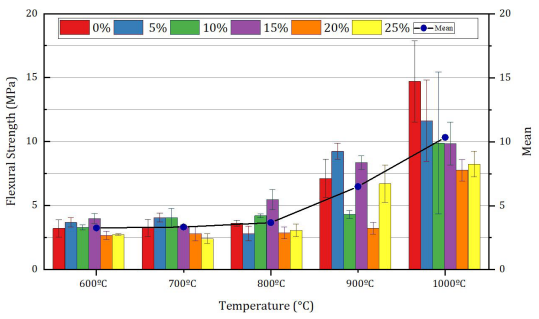


**Figure 7.** Flexural strength results.

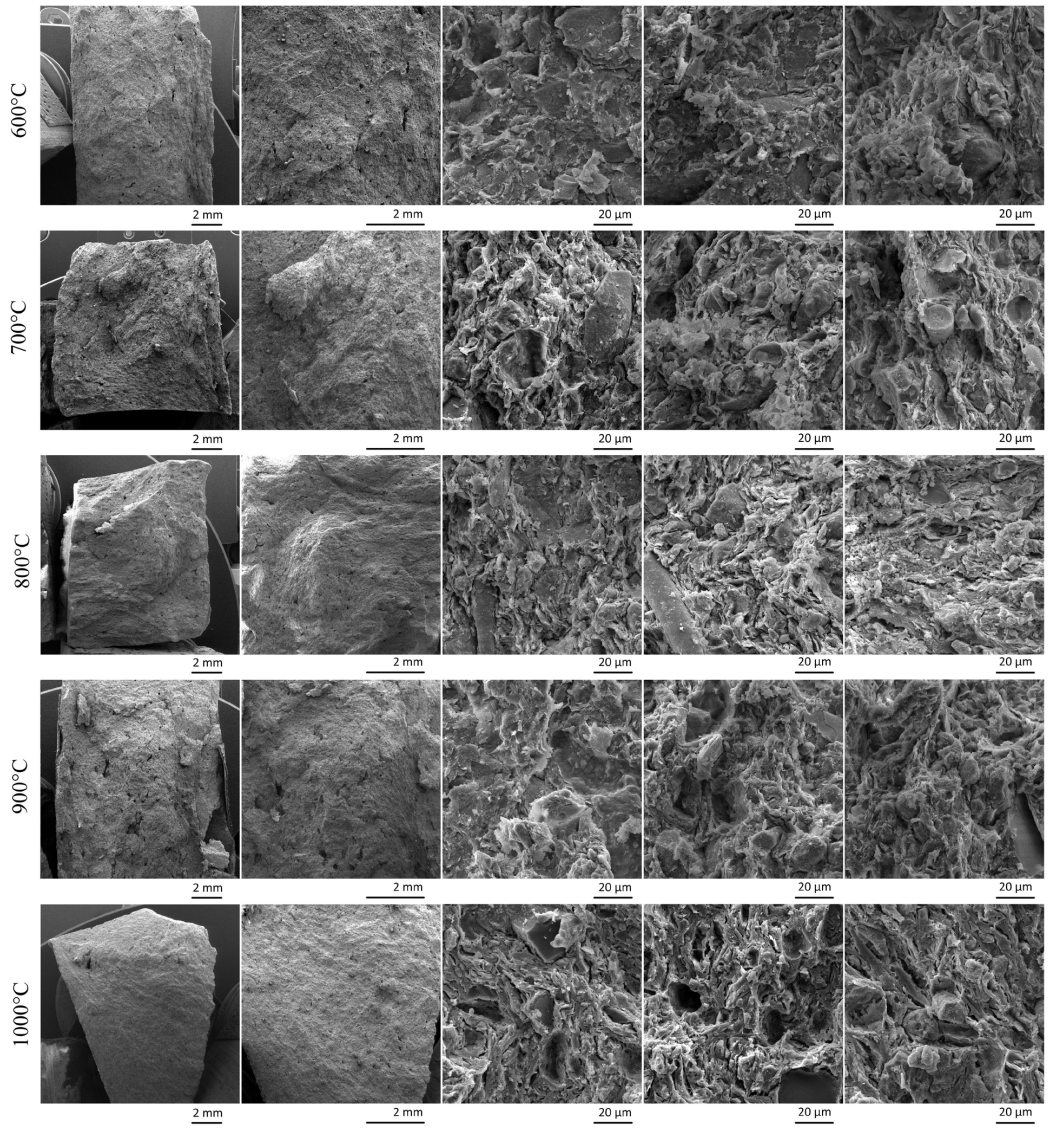


**Figure 8.** SEM micrographs of ceramic samples with 0% chamotte content sintered at different temperatures and magnifications: (a) 600°C, (b) 700°C, (c) 800°C, (d) 900°C, and (e) 1000°C.

dispersed throughout the matrix. At higher incorporation levels, particularly 20% and 25%, the presence of embedded, irregularly shaped particles becomes more evident, leading to a noticeable disruption in the microstructural uniformity. These morphological changes indicate that chamotte acts as a non-plastic inclusion, which interferes with the continuity of the clay matrix and contributes to increased surface roughness and textural heterogeneity.

At 0% chamotte, the matrix shows a uniform elemental distribution typical of pure clay, predominantly composed of silicon and aluminum. With the incorporation of 5% and 10% chamotte, localized increases in silicon and aluminum concentrations become evident, corresponding to the dispersed chamotte particles within the matrix. At higher incorporation levels, 15%, 20%, and 25%, the EDS spectra (not displayed) reveal a more heterogeneous composition, with distinct clusters enriched in silicon and aluminum, characteristic of chamotte-rich regions. These areas also suggest the presence of minor impurities, such as potassium or calcium, likely originating from the chamotte or the raw clay. These results are consistent with the SEM observations, reinforcing the interpretation of microstructural and compositional changes due to chamotte addition.

## *3.6. Thermal behavior of the test specimens*

All test specimens, regardless of formulation, exhibited fracture during the mechanical testing, revealing cross-sections characterized by rough, porous surfaces and noticeable color variations. These included the presence of black cores (commonly referred to as “black heart”), as well as beige to reddish-orange outer regions (Figure 10). Such variations are attributed to the sintering process and are influenced by both the composition and the firing temperature of the specimens.

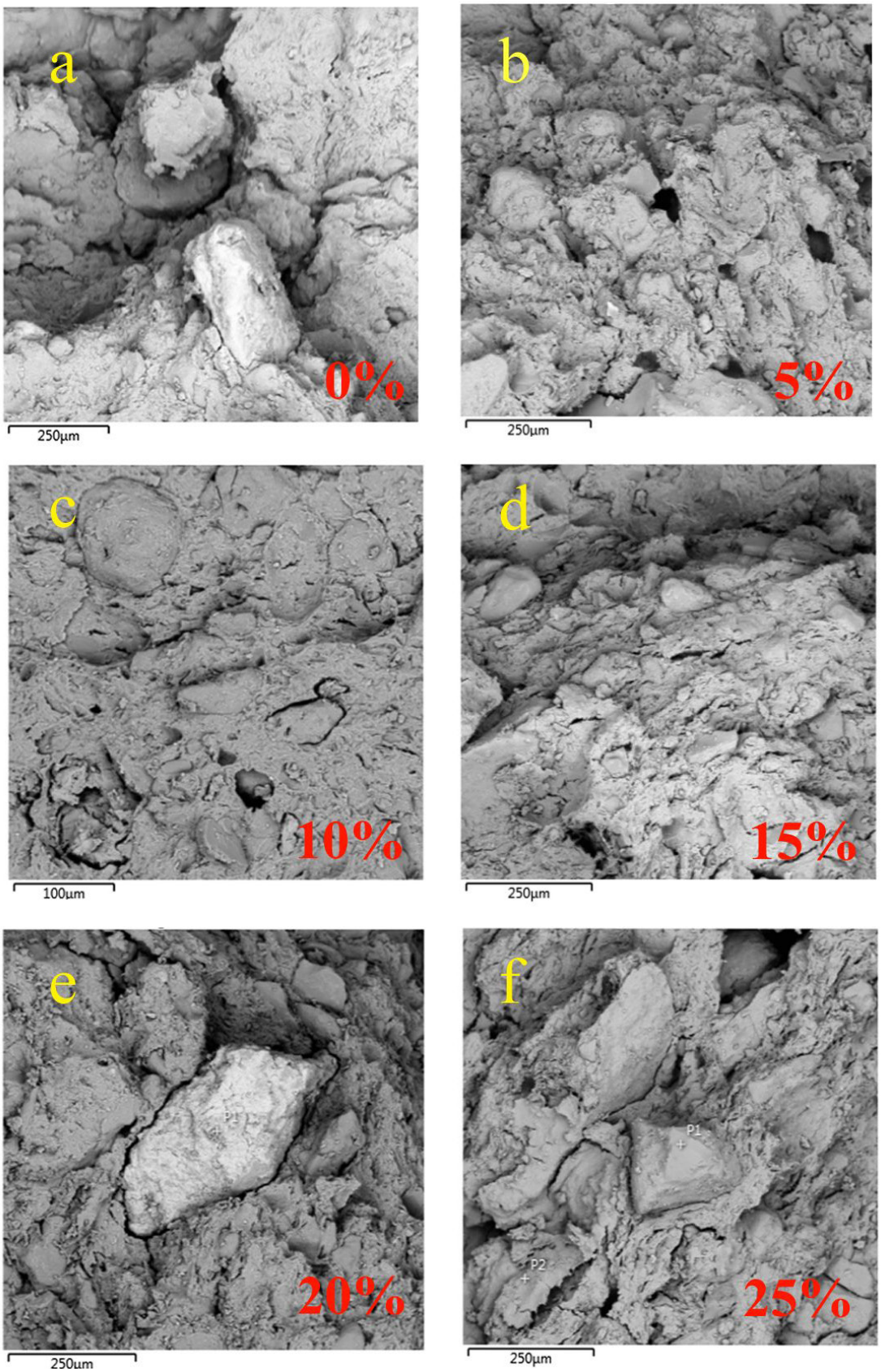


**Figure 9.** SEM micrographs of ceramic samples with varying chamotte content: a) 0%, b) 5%, c) 10%, d) 15%, e) 20%, and f) 25% chamotte incorporation.

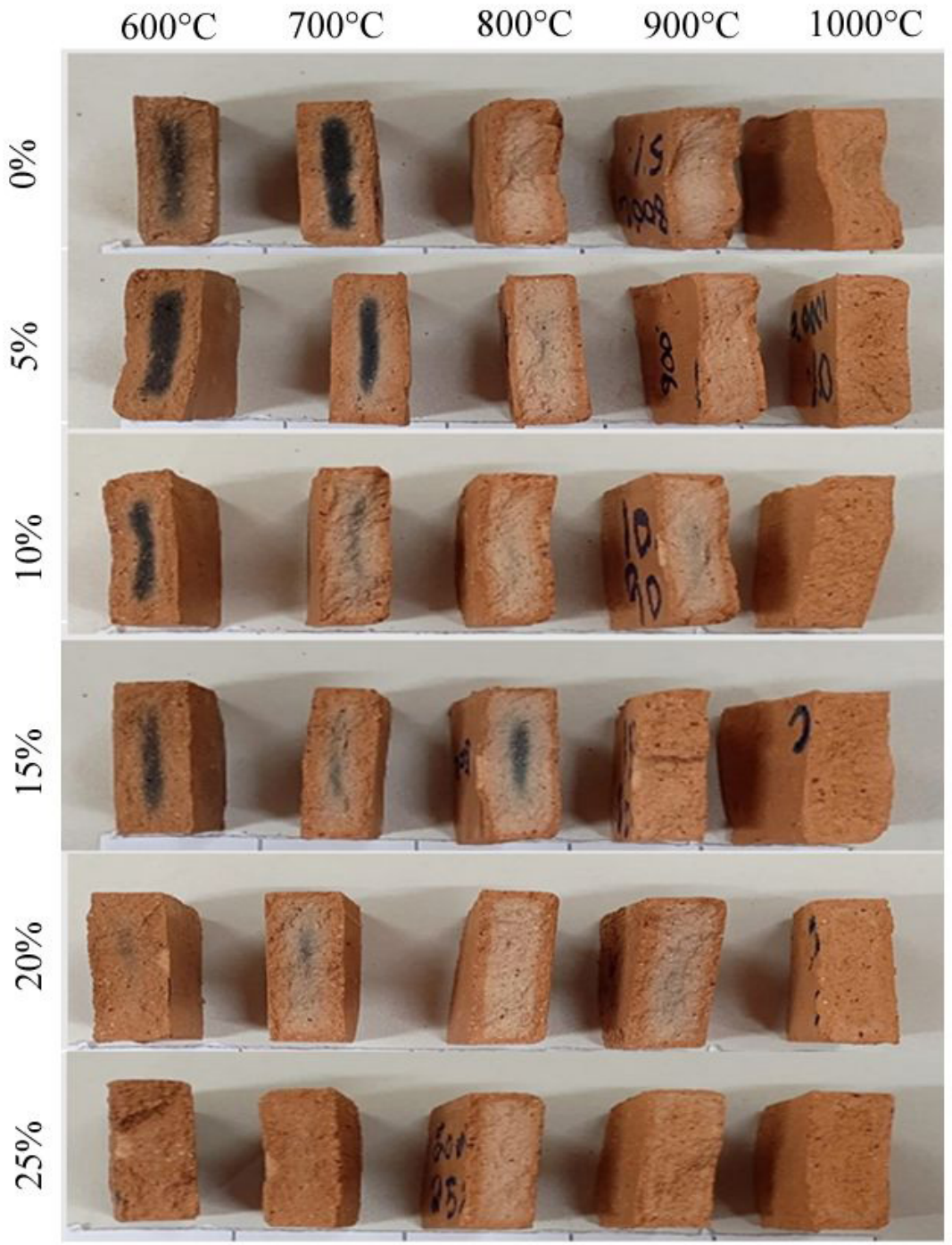


**Figure 10.** Thermal behavior of the fractured specimens.

The following observations can be made as the temperature increases:

- At lower temperatures, 600°C, a gradual formation of black cores occurs for samples with 0% to 20% chamotte. The black cores decreases as the chamotte content increases, becoming a homogeneous surface in color at 25% chamotte.
- In temperatures of 700°C, 800°C, and 900°C, the tendency is for black cores to appear in lower dosages and become beige with higher chamotte dosages, effectively diminishing the black cores, with clear influence from the addition of chamotte. It is observed that from 800°C onwards, the presence of black cores gradually disappears, and by 1000°C

they no longer appear. Therefore, the higher the temperature, the lower the chance of black core formation.

- At higher temperatures, 1000°C, homogeneous red-orange surfaces form for samples with 0% to 25% chamotte.

The following observations can be made as the chamotte percentage increases:

- With 0% chamotte, the black cores gradually decrease from 600°C to 1000°C,
- With 5% to 20% chamotte, the black cores gradually decrease from 600°C to 1000°C.
- With 25% chamotte, the surfaces are homogeneous in color from 600°C to 1000°C.

These results confirm that both increasing chamotte content and sintering temperature contribute significantly to the suppression of black cores formation in clay-based ceramics.

The presence of black cores, observed in the central part of ceramic test specimens, is the result of incomplete combustion of organic matter and the presence of iron compounds. This phenomenon is associated with increased porosity, as evidenced by the apparent porosity results in Figure 6b. Several factors that may contribute to the formation of the black cores, particularly in clay matrices with coarse granulometry, such as the sandy and gravel, like texture introduced by chamotte additions. Additionally, the presence of mass agglomerates with high moisture content, a significant proportion of volatile components (as indicated by a high Loss on Ignition, LOI ≈ 11%), and elevated iron oxide levels (chemically confirmed but not detected via XRD due to their amorphous or finely dispersed nature) play a critical role in this defect. The elevated LOI may result in the formation of pores that remain unfilled by fluxing oxides during sintering, thereby increasing water absorption and compromising mechanical strength. The presence of black cores not only exacerbates porosity but also contributes to the reduction in the structural integrity of the ceramic bodies.

The formation of black cores is an indicator that tends to influence mechanical strength and water absorption. As the pieces reduce the dark tone, better mechanical strength performance is observed, achieving good values at higher temperatures and poorer values when exposed to lower thermal conditions[43]. The formation of black cores, between 600°C and 800°C, consists of the reduction of $Fe^{+3}$ to $Fe^{+2}$, caused by the reducing environment generated by the formation of CO, a result of incomplete combustion of the originally present organic matter. Consequently, lower strengths are observed, which may lead to deformation of the pieces due to the presence of cracks. These effects are caused by the increase in pressure inside the test specimens, due to gas formation during firing.

## 4. Conclusions

The clay sample is composed of quartz and aluminosilicates derived from kaolinite and illite, exhibiting irregular morphology. Its chemical composition is predominantly $SiO_2$ (58.19%), $Al_2O_3$ (21.28%), and $Fe_2O_3$ (4.99%). The chamotte sample contains quartz, illite and K-feldspar, with a composition of $SiO_2$ (63.16%), $Al_2O_3$ (21.32%), and $Fe_2O_3$ (7.02%). Granulometric analysis classified the clay as a clayey silt and the chamotte as a silty sand. The high plasticity of the clayed silt sample confirms its suitability for traditional ceramic forming techniques, such as manual molding. The thermodynamic analysis revealed a mass loss of approximately 11% for the clay, in contrast to only 3.5% for the chamotte, indicating a higher volatile content in the clay. The kaolinite and illite phases undergo dehydration and dehydroxylation upon heating. Quartz remains thermally stable up to 1000 °C in both materials; however, kaolinite transforms into new phases such as spinel above 920 °C, contributing positively to the ceramic's final properties. Despite differences in granulometry, the mineralogical and chemical similarities between the clay and chamotte suggest a common geological origin and compatibility for blending at varied proportions.

All tested specimens exhibited flexural strengths exceeding the minimum threshold of 2.0 MPa, with a porous, rough, yet dense microstructure. These mechanical results are in accordance with the material's mineralogical composition, particularly the presence of illite and quartz, combined with adequate plasticity and porosity. Flexural strength showed only minor variations across temperatures ranging from 600°C to 800°C but increased significantly between 900°C and 1000°C. At 1000°C, flexural strength values exceeded 7.0 MPa, indicating suitability for applications such as red ceramic roofing tiles. It is suggested that ceramic bodies incorporating 5% to 15% chamotte and sintered at 900°C offer a viable balance between mechanical performance and energy efficiency, making them appropriate for artisanal ceramic production. Although optimal results were achieved at 1000°C, this temperature may not be practical for all manufacturing settings. Overall, the study provides valuable insights into phase transformations, microstructural evolution, and the enhancement of ceramic properties through chamotte incorporation during firing.

## 5. References

1. Reddy DHK, Lee SM, Kim JO. A review on emerging applications of natural sericite and its composites. World Appl Sci J. 2013;27(11):1514-23.
2. Nigay PM, Cutard T, Nzihou A. The impact of heat treatment on the microstructure of a clay ceramic and its thermal and mechanical properties. Ceram Int. 2017;43(2):1747-54.
3. Tite MS. Ceramic production, provenance and use: a review. Archaeometry. 2008;50(2):216-31.
4. IBGE: Instituto Brasileiro de Geografia e Estatística. Estatísticas do Cadastro Central de Empresas. Tabela 6449. Rio de Janeiro: IBGE; 2022.
5. IBGE: Instituto Brasileiro de Geografia e Estatística. Pesquisa Industrial Anual – Produto. Tabela 7752. Rio de Janeiro: IBGE; 2022.
6. Ceramic World Review. Investing in the future. Ceramic World Review. 2024;34(158):52-4.
7. Maged A, Abu El-Magd SA, Radwan AE, Kharbish S, Zamzam S. Evaluation insight into Abu Zenima clay deposits as a prospective raw material source for ceramics industry: remote sensing and characterization. Int J Sci Res. 2023;13:58.
8. Rosario SAS, Silva CAF. Clay physics: different ways of feeling and interpreting physical phenomena. Res Soc Dev. 2020;9(2):e294985306.
9. Santos DRS, Gomes GS, Sousa DJL, Vale SB, Paiva RS. The use of ceramic waste in the production of utilitarian ceramics in the municipality of Bragança-PA. In: Proceedings of the 28th Brazilian

National Meeting on Mineral Treatment and Extractive Metallurgy; 2019 Nov 4-8; Belo Horizonte, MG. Brazil. Proceedings. Belo Horizonte: UFMG-DEMIN; 2019. p. 31-39.
10. Pavlova IA, Getman AA, Farafontova EP. Technogenic raw materials in high alumina chamotte production. IOP Conf Series Mater Sci Eng. 2020;969:012031.
11. Trindade ACC, McNutt PF, Sood SS, Brandvold SS, Ozer A, Kriven WM. Optimizing the design parameters for chamotte particle-reinforced geopolymers. J Am Ceram Soc. 2024;107:6045-59.
12. Castro RJS, Soares RAL, Nascimento RM. Production of semi-porous ceramic tiles with the addition of roof tile chamotte. Matéria. 2012;17(4):11487.
13. Lopez-Perales JF, Sánchez-Rodríguez R, Suárez DD, Rodríguez EA. Fired electrical porcelain scrap (chamotte waste) recycling and reuse as an alternative raw material for sustainable porcelain stoneware production. J Clean Prod. 2024;434:140385.
14. Vieira CMF, de Souza ETA, Monteiro SN. Effect of grog incorporation in the processing and microstructure of red ceramic. Ceramica. 2004;50:254-60.
15. ABNT: Associação Brasileira de Normas Técnicas. NBR 6459:2016. Solo – Determinação do limite de liquidez. Rio de Janeiro: ABNT; 2016.
16. ABNT: Associação Brasileira de Normas Técnicas. NBR 7180:2016. Solo – Determinação do limite de plasticidade. Rio de Janeiro: ABNT; 2016.
17. ASTM: American Society for Testing and Materials. ASTM D4318 – 17: Standard Test Methods for Liquid Limit, Plastic Limit, and Plasticity Index of Soils. West Conshohocken: ASTM; 2018.
18. ABNT: Associação Brasileira de Normas Técnicas. NBR ISO 10545-3:2020. Revestimentos cerâmicos – Parte 3: Determinação da absorção de água, da porosidade aparente, da massa específica aparente e da massa específica real. Rio de Janeiro: ABNT; 2020.
19. ASTM: American Society for Testing and Materials. ASTM C326 – 09: Standard Test Method for Drying and Firing Shrinkages of Ceramic Whiteware Clays. West Conshohocken: ASTM; 2018.
20. Santos PS. Ciência e tecnologia de argilas. Sao Paulo: Edgard Blucher, 1989. (vol. 1).
21. Bergaya F, Lagaly G. General introduction: clays, clay minerals, and clay science. In: Bergaya F, Theng BKG, Lagaly G, editors. Handbook of clay science. New York: Elsevier; 2006. p. 1224. (vol. 1).
22. ASTM: American Society for Testing and Materials. ASTM C674-88: standard test methods for flexural properties of ceramic whiteware materials. West Conshohocken: ASTM; 2006.
23. Garcia E, Cabral M Jr, Quarcioni VA, Chotoli FF. Evaluation of the pozzolanic activity of heavy clay ceramic waste from main ceramic clusters of S. Paulo State, Brazil do Estado de S. Paulo. Ceramica. 2015;61(3):251-8.
24. Conconi MS, Morosi M, Maggi J, Zalba PE, Cravero F, Rendtorff NM. Thermal behavior (TG-DTA-TMA), sintering and properties of a kaolinitic clay from Buenos Aires Province, Argentina. Ceramica. 2019;65:227-35.
25. Acevedo NIA, Rocha MCG, Bertolino LC. Mineralogical characterization of natural clays from Brazilian Southeast region for industrial applications. Ceramica. 2017;63(366):620-45.
26. Savazzini-Reis A, Sagrillo VPD, Oliveira JN, Teixeira PG, Valenzuela-Diaz FR. Characterization and evaluation of ceramic properties with spherical and prismatic samples of clay used in red ceramics. Mater Res. 2017;20(6):915-22.
27. Gu X, Ling Y. Characterization and properties of Chinese red clay for use as ceramic and construction materials. Sci Prog. 2024;107(1):1-17.
28. Vieira CMF, Monteiro SN. Effect of grog addition on the properties and microstructure of a red ceramic body for brick production. Constr Build Mater. 2007;21(15):1754-9.
29. Wang H, Li C, Peng Z, Zhang S. Characterization and thermal behavior of kaolin. J Therm Anal Calorim. 2011;105:157-60.
30. Húlan T, Štubňa I, Shishkin A, Ozolins J, Csáki S, Bačík P, et al. Development of Young's modulus of natural illitic clay during heating and cooling stage of firing. Clay Miner. 2019;54:229-33.
31. Deju R, Cucos A, Mincu M, Tuca C. Thermal characterization of kaolinitic clay. Rom J Phys. 2021;66:904.
32. Earnest CM. Thermal analysis of selected illite and smectite clay minerals. Part II. Smectite clay minerals. In: Smykatz-Kloss W, Warne SSJ, editors. Thermal analysis in the geosciences. Berlin: Springer; 2005. p. 288-312. (Lecture Notes in Earth Sciences; vol. 38).
33. Keppert M, Pommer V, Šádková K, Krejsová J, Vejmelková E, Černý R, et al. Thermal activation of illitickaolinitic mixed clays. J Therm Anal Calorim. 2024;149:10533-44.
34. Gonidanga BS, Njoya D, Lecomte-Nana G, Njopwouo D. Phase transformation, technological properties and microstructure of fired products based on clay-dolomite mixtures. Journal of Materials Science and Chemical Engineering. 2019;7:1-14.
35. ABNT: Associação Brasileira de Normas Técnicas. NBR 7181:2016. Solo – Análise granulométrica. Rio de Janeiro: ABNT; 2016.
36. ASTM: American Society for Testing and Materials. ASTM D6913: Test Methods for Particle-Size Distribution (Gradation) of Soils Using Sieve Analysis. West Conshohocken: ASTM; 2009.
37. Rahman MF. Properties of fire clay after dressing and the effect of grog. In: Proceedings of the Global Engineering, Science and Technology Conference; 2012 Dec 28-29; Dhaka, Bangladesh. San Francisco: ISTES Organization; 2012. p. 28-9.
38. Teixeira SR, Souza SA, Moura CAI. Mineralogical characterization of clays used in the structural ceramic industry in west of S. Paulo State, Brazil. Ceramica. 2001;47(304):204-7.
39. Choo TF, Salleh MA, Kok KY, Matori KA, Rashid AS. A study on the utilization of coal fly ash derived grog in clay Ceramics. Materials. 2020;13(22):5218.
40. Ducman V, Škapin AS, Radeka M, Ranogajec J. Frost resistance of clay roofing tiles: case study. Ceram Int. 2011;37:85-91.
41. Jordan MM, Montero MA, Meseguer S, Sanfeliu T. Influence of firing temperature and mineralogical composition on bending strength and porosity of ceramic tile bodies. Appl Clay Sci. 2008;42:266-71.
42. Han J, Sun Q, Xing H, Zhang Y, Sun H. Experimental study on thermophysical properties of clay after high.temperature. Appl Therm Eng. 2017;111:847-54.
43. Smaniotto ALA, Rebelo WB. Estudo para a incorporação de rejeito fino de carvão mineral na massa da cerâmica vermelha. Revista Vincci. 2024;9(1):252-78.

## Data Availability

The authors declare that the data that support the conclusions on this paper are available on the publication itself (figures and tables).